Desalination and Water Treatment
www.deswater.com
doi: 10.1080/19443994.2014.893843

54 (2015) 2023–2035
May

Taylor & Francis
Taylor & Francis Group

Process modeling and thermodynamics and kinetics evaluation of Basic Yellow 28 adsorption onto sepiolite

Nalan Tekin*, Akif Şafaklı, Deniz Bingöl

Faculty of Art and Science, Department of Chemistry, Kocaeli University, Kocaeli 41380, Turkey, Tel. +90 262 303 203 1; email: nalan.tekin@kocaeli.edu.tr

Received 13 September 2013; Accepted 8 February 2014

ABSTRACT

The dye sorption of Basic Yellow 28 (BY 28) in an adsorption process was optimized by varying three independent factors (initial pH, temperature, and ionic strength) using a central composite design, which is an experimental design that is useful in response surface methodology. The quantitative relationship was measured between the amount of the adsorbed dye (q, mg g^{-1}) and the economical adsorbent, sepiolite, and the effect of initial pH, temperature, and ionic strength on the adsorption process was evaluated using the quadratic model. The model adequacy was tested by the analysis of variance, and the model was shown to be highly significant. The model showed that each of the independent factors was significant at the 5% significance level, revealing that the dye adsorption in the aqueous solution was affected by all three factors that were studied. The predicted maximum amount of adsorbed dye (31.54 mg g^{-1}) was found using a solution pH of 6, a temperature of 25°C, and an ionic strength of 0.00 mol L^{-1} within 30 min of contact time with the sepiolite. The activation energy was 19.11 J mol^{-1} for the adsorbed dye onto the sepiolite. The pseudo-second-order kinetic model appears to be the most efficient in describing the adsorption kinetics that were obtained from 20 to 60°C.

Keywords: Central composite design; Sepiolite; Basic Yellow 28; Adsorption kinetics

1. Introduction

The recent technological developments that have occurred in the textile and dye industries have made a positive contribution to the industries, but have also produced new and significant environmental problems [1]. The textile industry produces wastewater with heavy pollution levels. In the textile industry, approximately 40–65 L of wastewater is produced per kg of products. The textile dyes, which are used extensively in the textile industry, are a major pollutant in the textile effluents [2]. The textile industry produces 7×10^5 tons of dyes per year, and 10–15% of these dyes are released to the environment [1,3]. There are many structural varieties of dyes, such as acidic, basic, disperse, azo, diazo, anthraquinone-based, and metal complex dyes [4].

The cationic dyes, which are also known as basic dyes, are widely used in acrylic, nylon, silk, and wool dyeing processes. The basic dyes can cause allergic dermatitis, skin irritation, cancer, and mutations [5]. Therefore, the removal of the basic dyes from the process effluent is environmentally important. The most

*Corresponding author.

common methods for dye removal from aqueous solutions are aerobic and anaerobic microbial degradation, coagulation and chemical oxidation, solvent extraction, filtration, membrane separation, flotation, electrolysis, ion exchange, and sorption. Adsorption is one of the most suitable methods for dye removal because it is a simple and useful process [6].

The dyes can be effectively removed in an adsorption process, but the optimization of the process requires many experiments. Response surface methodology (RSM) is widely used for the optimization of process parameters, especially in adsorption processes. This methodology evaluates the interactions among the process variables through a relatively small number of experiments that can reduce time and cost [7–17]. The advantages of RSM over the other available design methods are that it involves a minimum number of experiments and aids in the evaluation of the relative significance of the variables that influence the process. RSM is useful for modeling, analysis, and optimization of responses that are influenced by several variables. There are numerous experimental designs that can be applied in the adsorption process to analyze and optimize the adsorption conditions. These designs include the central composite design (CCD), the Doehlert matrix, and the Box–Behnken design. In the CCD method, the primary effects and interactions among the variables are estimated.

Activated carbon is the most widely used adsorbent for dye removal because it has a high adsorption capacity and a large surface area for organic compounds. However, the use of activated carbon is typically limited due to its high cost [18]. Therefore, in recent years, many researchers have investigated alternative adsorbents that are efficient and economical for the removal of the dyes from wastewaters [19–23].

The use of clays in adsorption studies involving dye removal from wastewater is reported in the literature [24–26]. The sepiolite, which is one of the clay adsorbents, is a good alternative to activated carbon because it exhibits a high surface activity, a high porosity, and a high specific surface area [27]. The sepiolite is a phyllosilicate that contains a continuous two-dimensional tetrahedral sheet and differs from other layer silicates in that it lacks continuous octahedral sheets. The sepiolite is characterized by its tetrahedral–octahedral–tetrahedral (TOT) layer-fibrous structure that contains fragments of the TOT structures that extend along the axis [28]. The silanol groups on the surface of the sepiolite are typically accessible to organic species and act as neutral adsorption sites. In addition, certain isomorphic substitutions occur in the tetrahedral sheet of the lattice of the mineral form of sepiolite leading to negatively charged adsorption sites that are occupied by exchangeable cations. The sepiolite is a powerful sorbent for organic molecules and cations because of these characteristics [29].

The sepiolite is an efficient natural adsorbent that is obtained from local resources and from economical materials for the removal of hazardous dyes. Several studies that are related to the removal of dyes using sepiolite have been reported in the literature [10,30–34]. No studies were found in the literature by our research group that was related to Basic Yellow 28 (BY 28) adsorption onto the sepiolite using RSM. Therefore, in our present study, the sepiolite (Eskişehir, Turkey) was chosen as the sorbent and a basic dye (BY 28), which is used in Turkey's textile industry in Bursa was used as the model pollutant. The dependence of the adsorption capacity of the dye on contact time, concentration, temperature, adsorbent doses, and pH of the solution was studied. RSM was used for the optimization of the conditions for the maximum removal of the dye. The evaluation of the adsorption kinetics and thermodynamics was also performed.

2. Materials and methods

2.1. Materials

The sepiolite samples that were used in this study were obtained from Aktaş Lületaşı Co. (Eskişehir, Turkey). The chemical composition of the sepiolite determined by XRF is 53.47% SiO_2, 0.19% Al_2O_3, 0.16% Fe_2O_3, 0.71% CaO, 23.55% MgO, and 0.43% NiO and exhibited a 21.49 loss that was exhibited upon ignition. The clay sample was ground and sieved 75 μm size fraction. Then, it was dried at 105°C for 24 h and used for further experiments. The mineralogical compositions of the sepiolite samples were determined by a Rigaku Ultima IV X-ray diffractometer using copper K alpha (CuKα) radiation generated at 40 kV, 30 mA, and a scan speed of 1°/min. The XRD pattern of the sepiolite (Fig. 1) contains the sepiolite peaks at 6.97, 20.31, 27.85, 34.71, and 39.61 (2θ), which are the most characteristic peaks of the sepiolite [18,25]. On the basis of XRD peak intensities, the amount of the dolomite (at 30.94 (2θ)) appears to be small compared to the sepiolite.

The chemical and the electrokinetic characteristic of the sepiolite were described in previous articles [35–37]. The specific surface area of the sepiolite was 342 m^2 g^{-1}, as measured by the BET nitrogen

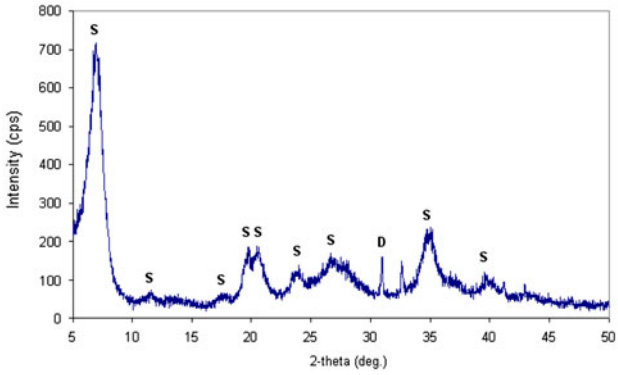

Fig. 1. The XRD pattern of the sepiolite (S: sepiolite, D: dolomite).

adsorption technique using the Micromeritics FlowSorb II-2300 equipment. The cationic exchange capacity (CEC) of the sepiolite using the ammonium acetate method was determined to be 25.0 meq/100 g. The sepiolite had an isoelectric point at a pH˚of approximately 6.6. The BY 28 (purity, 95%) textile dye was obtained from Dystar, Turkey, and was used without further purification. The structure of the dyes and their properties are given in Fig. 2 and Table 1.

2.2. The adsorption experiments

For the experiments on the adsorption kinetics, a 1.25 sepiolite sample was added to 2 L of a BY 28 solution at the desired ionic strength, temperature, and pH. The initial concentration of the BY 28 solution was 4×10^{-5} mol L^{-1}. A preliminary experiment showed that the adsorption process reached the equilibrium concentration after approximately 60 min. The mixture was continuously agitated by a mechanical stirrer at 400 rpm for 60 min.

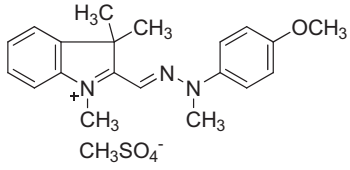

Fig. 2. Molecular structure of BY 28.

Table 1
Property of BY 28 dye

Commercial name	Astrazon Gelb GLE
λ_{max} (nm)	438.79
Type	Cationic
M_W (g mol^{-1})	433.52
Azo group	1
Solubility	90˚C, 80 g/L; 60˚C, 60 g/L; 30˚C, 40 g/L
pH stability	3–10

The effect of the solution pH on the dye removal was studied in the pH range from 3 to 9. The pH was adjusted using 0.1 mol L^{-1} HCl and 0.1 mol L^{-1} NaOH solutions using a NeoMet pH-200 l pH meter with a combined pH electrode. The pH meter was standardized with NBS buffers before each measurement was obtained. The effect of the ionic strength on the adsorption rate was studied using an NaCl concentration range of 0.0–0.1 mol L^{-1}. The experiments were performed at temperatures ranging from 20 to 60˚C in a constant temperature bath. Four milliliters of the samples was removed from the adsorption system at certain time intervals. The samples were centrifuged for 15 min at 4,000 rpm, and the dye concentration remaining in the supernatant solution was determined using a UV–Vis spectrophotometer (Shimadzu UV-2450) at the wavelength of 438.79 nm.

At any time t, the adsorbed dye amount, q_t, was calculated from Eq. (1):

$$q_t = (C_0 - C_t)\frac{V}{m} \quad (1)$$

where C_0 is the initial concentration of the BY 28 solution, and C_t is the liquid-phase concentration of the BY 28 solution at any time, t (mg L^{-1}); m is the sepiolite mass (g); V is the volume of the BY 28 solution (L); and q_t is the BY 28 concentration that is adsorbed on the sepiolite at any time, t (mg g^{-1}).

2.3. The experimental design

The analysis of the statistical quality of the experimental results prior to their evaluation is essential because if the quality of the results is not statistically significant, then the analysis of the design will produce misleading conclusions [38]. The experimental design involves the estimation of the coefficients in a mathematical model that predict the response and test the adequacy of the model. The response model may be expressed using Eq. (2):

$$y = f(X_1.X_2.X_3...X_n) \pm \varepsilon \quad (2)$$

where y is the response, f is the response function, X_i represents the independent variables, and ε is the

Table 2
Experimental range and levels of independent variables

Factors	Range and levels				
	−α (−1.68)	−1	0	+1	+α (+1.68)
X_1: Initial pH	3.0	4.2	6.0	7.8	9.0
X_2: Temperature (T), ℃	20	28	40	52	60
X_3: Ionic strength (I), mol L^{-1}	0.00	0.02	0.05	0.08	0.10

experimental error. The response function, f, depends on the nature of the relationship between the response and the independent variables. The RSM aims to at approximate the value of f using a suitable polynomial in a region of the independent process variables [39].

The experimental data can be evaluated for the analysis of the responses (y) using the following second-order polynomial equation as a function of the independent variables (Eq. (3)):

$$y = \beta_0 + \sum_{i=1}^{k} \beta_i x_i + \sum_{i=1}^{k} \beta_{ii} x_i^2 + \sum_{1 \le i \le j}^{k} \beta_{ij} x_i x_j + \varepsilon \quad (3)$$

where x_1, x_2, … x_k are the input variables that have an influence on the response y; β_0, β_i ($i = 1, 2, \ldots k$) β_{ii}, *and* β_{ij} ($i = 1, 2, \ldots k$; $j = 1, 2, \ldots k$) are intercept, linear, quadratic, and interaction constant coefficients, respectively, and ε is a random error [40]. The CCD method was used to develop the response model and the desirability function in the optimization of the affecting parameters (initial pH, temperature, and ionic strength) to produce the highest amount of adsorbed dye. The levels that are defined for the parameters are listed in Table 2 and were selected according to preliminary experiments.

Table 3
CCD matrix of three variables in coded and actual levels along with the observed response for the adsorption of BY 28 dye

Run	Coded and actual level of variables			q_e (mg g^{-1})
	pH	T (℃)	I (mol L^{-1})	
1	4.2 (–1)	28 (–1)	0.02 (–1)	30.91
2	7.8 (+1)	28 (–1)	0.02 (–1)	31.05
3	4.2 (–1)	52 (+1)	0.02 (–1)	31.36
4	7.8 (+1)	52 (+1)	0.02 (–1)	30.71
5	4.2 (–1)	28 (–1)	0.08 (+1)	30.02
6	7.8 (+1)	28 (–1)	0.08 (+1)	29.46
7	4.2 (–1)	52 (+1)	0.08 (+1)	30.86
8	7.8 (+1)	52 (+1)	0.08 (+1)	30.77
9	3.0 (–1.68)	40 (0)	0.05 (0)	30.91
10	9.0 (+1.68)	40 (0)	0.05 (0)	30.60
11	6.0 (0)	20 (–1.68)	0.05 (0)	30.62
12	6.0 (0)	60 (+1.68)	0.05 (0)	31.66
13	6.0 (0)	40 (0)	0 (–1.68)	31.23
14	6.0 (0)	40 (0)	0.10 (+1.68)	31.09
15	6.0 (0)	40 (0)	0.05 (0)	31.01

The factorial design matrix and the observed response (q_e, mg g^{-1}) of the adsorption of the BY 28 dye that was obtained for each factorial experiment are given in Table 3, where the levels are those specified in Table 2. The q_e value was determined to be average, with three replicates for each of these experiments. The order in which the experiments were conducted was randomized to avoid systematic errors, and the statistical program package, *Minitab-16*, was used for the analysis of the data that were obtained and for the estimation of the coefficient of the regression equation.

3. Results and discussion

3.1. Statistical analysis

The RSM was used to investigate the influence of the variables (initial pH, temperature, and ionic strength) on the amount of the dye that was adsorbed and to find the most suitable combination of the variables that would result in a maximum amount of adsorbed dye. The analysis of variance (ANOVA) model was used for the graphic analysis of the data to obtain the interaction between the process variables and the responses. In addition, with the aid of the model, the optimal response can be estimated by calculating the derivatives of the model. The terms of the fit polynomial model were evaluated by the P-value (probability) with a 95% confidence level and by the ANOVA model (Table 4).

The probability values of less than 0.05 are considered to be significant evidence that the coefficient is not zero. Any p-values that is lower than 0.05 indicate that the model and the model terms are statistically significant. All of the linear (X_1, X_2, X_3), the squares of the pH (X_1^2), and the $T \times I$ (X_2X_3) interaction coefficients ($p < 0.05$) were significant at the 5% significance level for the amount of the adsorbed dye (q_e). Table 4 shows the statistical analysis of the model that was performed to evaluate the ANOVA.

Table 4
Estimated effects and coefficients for q_e (mg g^{-1}) at coded units

Term	Coefficients	Standard error	*T*-value	*p*-value
Constant	31.03	0.0691	449.13	0.000
pH (X_1)	–0.12	0.0458	–2.68	0.010
T (X_2)	0.30	0.0458	6.44	0.000
I (X_3)	–0.23	0.0458	–5.05	0.000
pH × pH (X_1^2)	–0.17	0.0446	–3.81	0.000
T T (X_2^2)	–0.04	0.0446	0.79	0.434
$I \times I$ (X_3^2)	–0.03	0.0446	–0.61	0.548
pH × T (X_1X_2)	–0.04	0.0599	–0.68	0.501
pH × I (X_1X_3)	–0.02	0.0599	–0.31	0.757
$T \times I$ (X_2X_3)	0.26	0.0599	4.28	0.000

Values for the reduced model with significant coefficients: S = 0.04819, PRESS = 0.1552, R^2= 98.65%, R^2(pred)= 98.33%, R^2(adj)= 98.52%

Analysis of variance for suggested quadratic model

Source	DF	SS	MS	*F*-ratio	*p*-ratio
Regression	5	9.147	1.829	787.8	0.000
Linear	3	6.385	2.129	916.4	0.000
Square	1	1.188	1.188	511.4	0.000
Interaction	1	1.574	1.574	677.6	0.000
Residual error	54	0.125	0.002		
Total	59	9.273			

Notes: S: standard deviation (SD), PRESS: predicted residual sums of squares, R^2: coefficient of determination, R^2(pred): predicted coefficient of determination, R^2(adj): adjusted coefficient of determination, DF: degrees of freedom, SS: sum of square, MS: mean of square.

A quantitative reduced model equation for the adsorbed dye amount (q_e) can be expressed using coded units in terms of the statistically significant effects, as Eq. (4):

$$q_e(\text{mg g}^{-1}) = 30.98 - 0.12\ X_1 + 0.30\ X_2 - 0.23\ X_3 - 0.16\ X_1^2 + 0.26\ X_2X_3 \quad (4)$$

The quality of the fitted model was evaluated by the coefficient of determination, R^2. This value represents the percentage of the response variation that is explained by the model, that is, how well the model fits the data. An R^2 value that is larger than 0.9 is typically required for an adequate approach [41]. The value of the adjusted R^2 (98.52%) suggested that only approximately 1.48% of the total variation cannot be explained by the model. A model is valid when it has good predictability [42]. The low value for *PRESS* (0.1552) and the high predicted R^2 value (98.33%) showed the high predictive ability of the model.

This function describes how the experimental variables and their interactions influence the BY 28 adsorption. Temperature (X_2) had the greatest effect on q_e followed by temperature–ionic strength interaction (X_2X_3), ionic strength (X_3), and pH (X_1). The positive values of these effects reveal that the increase in these parameters increased q_e. Conversely, the negative values of the effects decreased the response (q_e). The effects of pH and ionic strength are negative, that is, a decrease in q_e is observed when the factor changes from low to high. In addition, pH had a smaller effect on q_e than temperature and ionic strength. The slight effect of pH on dye removal as well as the stable final pH of the suspensions is mainly determined by the nature of the large pH buffer capacity of the sepiolite suspension.

Therefore, pH is not a critical limiting factor in pursuing a high efficiency of dye removal using sepiolite, and no rigid pH control is needed. That is an important advantage for sepiolite application because dye removal using conventional adsorbents or chemical coagulants is strongly pH-dependent; therefore, an optimal pH condition should be maintained to achieve a satisfactory result [43].

Increasing the ionic strength of the solution causes a decrease in the adsorption of BY 28 onto sepiolite. The amount of adsorbed BY 28 by the sepiolite sample decreases with the increase in the ionic strength of the medium. This result can be explained by the reduction in the positive surface potential of the sepiolite sample [44].

Increasing the temperature causes an increase in the adsorption of BY 28 onto sepiolite. Increasing the temperature increases the rate of diffusion of adsor-

bate molecules across the external boundary layer and in the internal pores of the adsorbent particle due to the decrease in the viscosity of the solution. In addition, changing the temperature will change the equilibrium capacity of the adsorbent for a particular adsorbate [45]. This type of temperature dependence of the adsorbed amount of the dyes may reflect the increase in the case, in which the dye penetrates into the sepiolite because of its larger diffusion coefficient. In fact, a possible mechanism of interaction is the reaction between the hydroxyl end groups of the sepiolite and the cationic group in the dye molecules; such a reaction could be favoured at higher temperatures [46].

A display of the predicted model equation can be obtained by plotting the surface response. The three-dimensional surface plots and their respective contour plots were obtained for the adsorbed dye amount based on the effects of the three factors (pH, temperature, and ionic strength) at five levels. To represent the response surface graphically, the amount of the adsorbed dye (mg g^{-1}) was plotted vs. the pH levels, the temperature and the ionic strength. Fig. 2 shows the combined effect of temperature and ionic strength with a significant interaction coefficient (X_2X_3) on the adsorption of the dye at a constant initial pH (5). According to the main effects of each parameter on the dye adsorption, increasing the temperature causes the increase in the adsorption of BY 28 onto sepiolite, but according to interaction effects for temperature, and ionic strength, an increase in the temperature within the experimental range showed a slight decrease in the amount of adsorbed dye. The increase in the temperature complicates the sorbate transport within the pores of the sorbent, which may explain the decrease in adsorption with the increasing temperature. In addition, the adsorption of the dye on the sepiolite decreased upon addition of small quantities of salt. In addition, Fig. 3 shows that at low temperatures and at a pH of 5 the amount of the adsorbed dye in the ionic strength range of 0.00–0.10 mol L^{-1} NaCl decreased with an increase in ionic strength. When there are attractive electrostatic forces between the adsorbent surface and the adsorbate, as in this system, then an increase in the ionic strength will decrease the adsorption capacity.

The two-dimensional contour plot provides information so that predictions can be made for combinations that are not experimentally evaluated. The contour plot, presented in Fig. 4, shows how a response variable relates to two factors based on a model equation. This plot shows that the amount of the adsorbed dye is related to the temperature and the ionic strength at pH 5. The maximum adsorption on

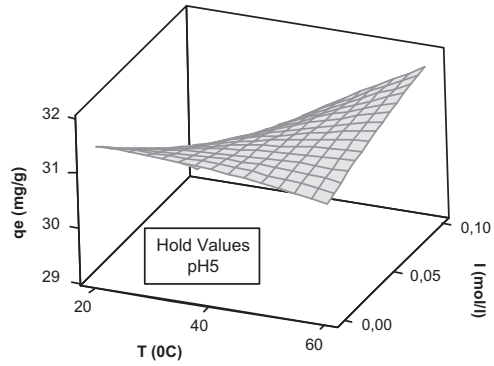

Fig. 3. The surface plots obtained using COD.

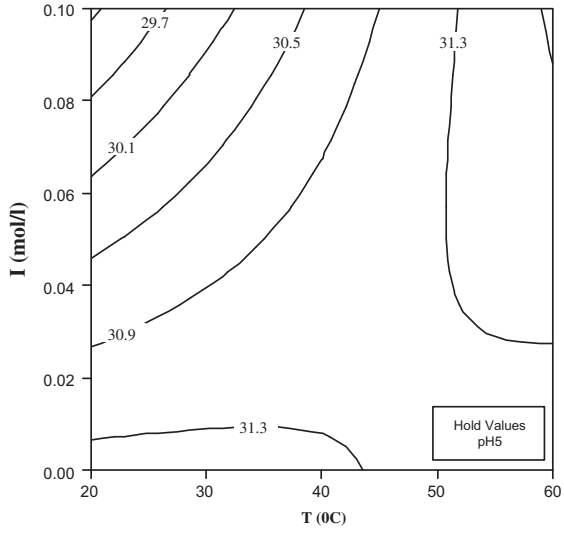

Fig. 4. The contour plots obtained using COD.

the plot was found at a low temperature and a low ionic strength. However, the experimental maximum adsorption was found at the highest temperature and the highest ionic strength due to the interaction effect of the temperature and ionic strength on the adsorption of the dye.

3.2. Adsorption kinetics

Many mathematical models are used to describe the adsorption kinetics. The first-order reaction rate model, known as the Lagergren kinetic equation, is one of those mathematical models. The pseudo-first-order equation is generally expressed according to Eq. (5) [47,48]:

$$\frac{dq_t}{dt} = k_1(q_e - q_t) \tag{5}$$

After integrating and applying the boundary conditions for $q_t = 0$ at $t = 0$ and $q_t = q_t$ at $t = t$, the linear form of the pseudo-first-order model is given in Eq. (6):

$$\ln(q_e - q_t) = \ln q_e - k_1 t \quad (6)$$

where k_1 is the rate constant (mg^{-1}), q_e is the amount of the BY 28 that was adsorbed at equilibrium (mg g^{-1}), and q_t is the amount of the BY 28 that was adsorbed at time t (mg g^{-1}).

The pseudo-second-order equation is expressed according to Eq. (7) [47,48]:

$$\frac{t}{q_t} = \frac{1}{k_2 q_e^2} + \frac{1}{q_e} t \quad (7)$$

where k_2 is the rate constant of the pseudo-second-order model for the adsorption process (g mg^{-1} min^{-1}).

To obtain the rate parameters, the plots of ln (q_1−q_t) vs. t, t/q_t vs. t, and q_t vs. $t^{1/2}$ were used for the Lagergren first-order model, the pseudo-second-order model, and the intra-particle diffusion model, respectively.

The kinetic parameters of the BY 28 adsorption onto the sepiolite were calculated using these plots, and the parameters are shown in Table 5. The coefficient of determination, R^2, for the pseudo-second-order adsorption model has a high value (>0.99), which indicates that BY 28 adsorption onto sepiolite samples follows the pseudo-second-order rate expression. According to the literature, the pseudo-second-order kinetic model includes different sorption mechanisms, such as surface complexation and ion exchange. The model is based on the assumption that the rate-limiting step may be chemical sorption or chemisorption involving valence forces through the sharing or exchange of electrons between the sorbent and the sorbate [47,49]. Similar results were observed in the adsorption of cationic dyes onto sepiolite [5,6,30,45].

Because temperature has the greatest effect on q_e, the effect of temperature on the adsorption kinetics was also studied. Table 6 lists the results of the rate constant studies for different temperature by the pseudo-first-order and pseudo-second-order models. As shown in Table 6, when the temperature increases from 20 to 60 °C, the second-order kinetic rate constant, k_2, increases from 3.74×10^{-2} to 9.99×10^{-2} g/mg min. This finding suggests that a high temperature favors BY 28 removal by adsorption onto sepiolite.

The pseudo-first-order and pseudo-second-order kinetic models may not reveal information on the diffusion mechanism in the adsorption process; therefore, the kinetic results from this study were analyzed using the intra-particle diffusion model [50]. Generally, any sorption process involves three main successive transport steps, which are (i) film diffusion, (ii) intra-particle or pore diffusion, and (iii) sorption onto interior sites. Among the three steps, the last step is

Table 5
The results of the kinetic analysis of the adsorption experiments

Run	q_e (mg g^{-1})	Results			
		Lagergren first-order rate expression		Pseudo-second-order kinetic model equation	
		R_1^2	$k_1 \times 10^1$ (min^{-1})	R_2^2	$k_2 \times 10^2$ (g mg^{-1} min^{-1})
1	30.91	0.9034	0.679	0.9999	3.97
2	31.05	0.9505	1.39	0.9999	5.98
3	31.36	0.9680	1.63	0.9999	7.24
4	30.71	0.9852	1.47	0.9999	9.48
5	30.02	0.9309	0.840	0.9999	4.74
6	29.46	0.9620	1.17	0.9999	5.17
7	30.86	0.9693	1.46	0.9999	9.87
8	30.77	0.8704	0.673	0.9999	7.99
9	30.91	0.9854	0.890	0.9999	3.95
10	30.60	0.9908	1.41	0.9999	7.67
11	30.62	0.9571	0.673	0.9999	3.74
12	31.66	0.9903	1.49	0.9999	9.99
13	31.23	0.9613	1.72	0.9999	6.05
14	31.09	0.9464	1.01	0.9999	6.36
15	31.01	0.8979	0.122	0.9999	6.16

Table 6
The results of the kinetic analysis of the adsorption experiments at various temperatures

T (℃)	Lagergren first-order rate expression ($k_1 \times 10^1$) (min^{-1})	R^2	Pseudo-second-order kinetic model equation ($k_2 \times 10^2$) ($g\,mg^{-1}\,min^{-1}$)	R^2	Intraparticle diffusion equation ($mg\,g^{-1}\,min^{-1/2}$)		R^2	
					($k_{int,1}$)	($k_{int,2}$)	($k_{int,1}$)	($k_{int,2}$)
20	0.673	0.9571	3.74	0.9999	1.997	0.368	0.9817	0.9687
30	1.15	0.9867	5.01	0.9999	1.949	0.243	0.9730	0.7509
40	0.122	0.8979	6.16	0.9999	1.803	0.280	0.9919	0.8958
50	0.946	0.9417	7.39	0.9999	1.746	0.215	0.9629	0.8932
60	1.49	0.9903	9.99	0.9999	1.619	0.185	0.9349	0.8869

considered negligible, as it is assumed to be rapid, and the rate of sorption is controlled by either film diffusion or pore diffusion depending on which step is slower [51]. Weber and Morris [52] stated that if intra-particle diffusion is the rate-controlling factor, uptake of the adsorbate varies with the square root of time. Thus, rates of adsorption are usually measured by determining the adsorption capacity of the adsorbent as a function of the square root of time [53].

The initial rate of the intra-particle diffusion can be obtained using Eq. (8) [48]:

$$q_t = f(t^{1/2}) \tag{8}$$

The rate parameter (k_{int}) for the intra-particle diffusion can be defined by Eq. (9):

$$q_t = k_{int} t^{1/2} + C \tag{9}$$

where k_{int} is the intra-particle diffusion rate constant [$(mg(g\,min^{1/2}))^{-1}$]. The slope of the linear portion of the curve in the plot of q_t vs. $t^{1/2}$ gives the rate constant that is controlled by intra-particle diffusion.

The intra-particle diffusion plots for the effect of temperature on the adsorption of BY 28 onto sepiolite are shown in Fig. 5. From this figure, it is observed that there are two linear portions. The intra-particle diffusion constants $k_{int,1}$ and $k_{int,2}$ ($mg/g\,min^{1/2}$) are calculated using Eq. (9) from the slope of the corresponding linear region of Fig. 5. The calculated $k_{int,1}$ and $k_{int,2}$ values for different solution temperatures are given in Table 6. The $k_{int,1}$ and $k_{int,2}$ express the diffusion rates of the different stages in the adsorption [54]. Considering a solid–liquid adsorption process, the adsorbate transfer is characterized by either boundary layer diffusion or intra-particle diffusion, or a combination of both [5,6]. Fig. 5 shows two linear portions. The first part is attributed to boundary layer diffusion (external mass transfer), whereas the final linear part indicates the effect of intra-particle diffusion. The intercept value gives an idea about the boundary layer thickness, such as the larger the intercept is the greater the boundary layer effect [6,18,30]. The slope of the linear portion indicates the rate of the adsorption. The lower slope corresponds to a slower adsorption process. If these lines pass through the origin, then intra-particle diffusion is the rate-controlling step. When the plots do not pass through the origin, then intra-particle diffusion is not the only rate-limiting step, and other kinetic models may also control the rate of adsorption, all of which may be operating simultaneously [6]. In this study, neither plot passed through the origin. It was suggested that this occurs when external diffusion is dominant and intra-particle diffusion is not a rate-limiting step. When the reaction orders and adsorption mechanisms were compared, similar results were found for basic dyes on sepiolite in the literature [6,30,45].

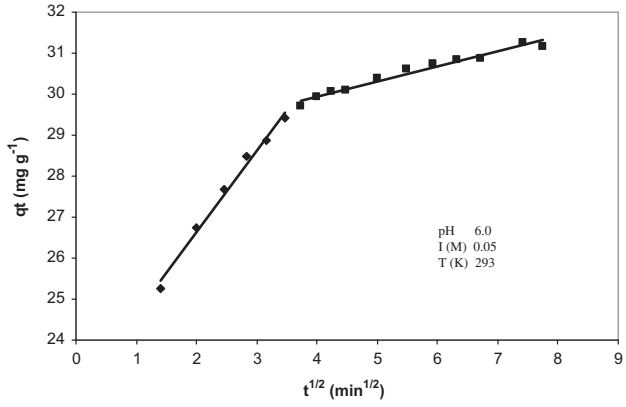

Fig. 5. Intra-particle diffusion plots for the adsorption of BY 28 onto sepiolite.

3.3. The adsorption isotherms

The adsorption isotherm is critical in optimizing the use of adsorbent because it can be used to not only assess the adsorption capacity of the adsorbent but can also describe how the adsorbate interacts with the adsorbent [55]. The Langmuir and Freundlich isotherm models were applied to simulate the experimental data.

The Langmuir model assumes that a monomolecular layer is formed when adsorption occurs without any interaction between the adsorbed molecules. Generally, the Langmuir isotherm [56] is represented in the linear form, which is expressed in Eq. (10):

$$\frac{C_e}{q_e} = \frac{1}{q_m K_L} + \frac{C_e}{q_m} \tag{10}$$

where C_e is the equilibrium concentration of the BY 28, K_L is the Langmuir constant ($L\,mg^{-1}$) that is related to the free energy of adsorption, q_m ($mg\,g^{-1}$) is the monolayer capacity of the BY 28, and q_e ($mg\,g^{-1}$) is the amount of the adsorbed BY 28. The slopes and intercepts of the straight lines of the plot of C_e/q_e vs. C_e are used for the calculation of q_m and K_L.

The Freundlich model involves equilibrium on a heterogeneous surface where the sorption energy is not homogeneous for all sorption sites. The Freundlich isotherm is expressed in the following equation [57]:

$$q_e = K_F C_e^{1/n} \tag{11}$$

The logarithmic form of Eq. (11) is expressed in Eq. (12):

$$\ln q_e = \ln K_F + \frac{1}{n} \ln C_e \tag{12}$$

where $(1/n)$ is the adsorption intensity, and K_F is an approximate indicator of the adsorption capacity. The K_F and $(1/n)$ values can be determined from the linear plot of ln q_e vs. ln C_e.

Freundlich parameters (K_F and n) indicate whether the nature of adsorption is either favorable or unfavorable. The intercept and slope are indicators of adsorption capacity and intensity, respectively.

The parameters of the Langmuir and Freundlich isotherm models that were determined are shown in Table 7. The Langmuir model fits the experimental data (correlation coefficient, $R^2 > 0.99$) better than the Freundlich model (correlation coefficient, $R^2 < 0.99$). Thus, the sorption behavior of BY 28 onto sepiolite is considered to be representative of sorption onto a monolayer [6]. Additionally, both q_L and K_L increased with increasing temperature, indicating that bonding between the dye and the active sites of the adsorbent become strong at higher temperature and the adsorption process is endothermic. High temperatures increased the kinetic energy of the dye and therefore enhanced the mobility of the dye ions. This led to a higher chance of the dye being adsorbed onto the adsorbent and an increase in its adsorption capacity. This agreed well with the findings in literature [58].

The Freundlich parameters at different temperatures for the adsorption of BY 28 onto sepiolite are shown in Table 7. The Freundlich constant K_F indicates the adsorption capacity of the adsorbent. The other Freundlich constant n is a measure of the deviation from the linearity of the adsorption. If a value for n is equal to unity the adsorption is linear. But if a value for n is below unity, this implies that the adsorption process is chemical, but a value for n is above unity, adsorption is favorable as a physical process [31]. The highest value of n at equilibrium is at 60℃, which represents favorable adsorption at high temperature.

3.4. The activation thermodynamic parameters

The K_L value is the equilibrium constant and is dependent on the temperature. Therefore, this value can be used to estimate certain thermodynamic parameters, such as the standard free energy (ΔG^*), the enthalpy (ΔH^*), and the entropy (ΔS^*), all of which are associated with the adsorption process. The thermodynamic parameters for the adsorption process were determined by Eqs. (13) and (14):

$$\Delta G^* = -RT \ln K_L \tag{13}$$

$$\ln K_L = -\frac{\Delta G^*}{RT} = -\frac{\Delta H^*}{RT} + \frac{\Delta S^*}{R} \tag{14}$$

The plot of ln K_L as a function of $1/T$ (Fig. 6) yields a straight line. The ΔH^* and ΔS^* values were calculated using the slope and the intercept, respectively, from in this plot. The linear regression coefficient was 0.9968.

The Gibbs free energy of adsorption (ΔG^*) can be found using the following equation:

$$\Delta G^* = \Delta H^* - T\Delta S^* \tag{15}$$

The results obtained using Eqs. (13)–(15) are given in Table 8. The ΔG^* values were negative for all of the temperatures that were studied, indicating that the adsorption process was spontaneous. The change in

Table 7
Isotherm constants for BY 28 adsorption onto sepiolite (at $I = 0.05$ mol L^{-1} NaCl and pH 6)

T (℃)	Langmuir isotherm			Freundlich isotherm		
	q_m (mg g^{-1})	K_L (L mg^{-1})	R^2	n	K_F	R^2
20	25.19	5.84	0.9995	11.36	30.14	0.9777
30	25.97	8.19	0.9995	13.28	29.92	0.9497
40	26.81	11.66	0.9954	15.90	29.87	0.9892
50	27.62	14.48	0.9990	18.87	30.38	0.9420
60	28.01	19.83	0.9960	22.08	30.10	0.9441

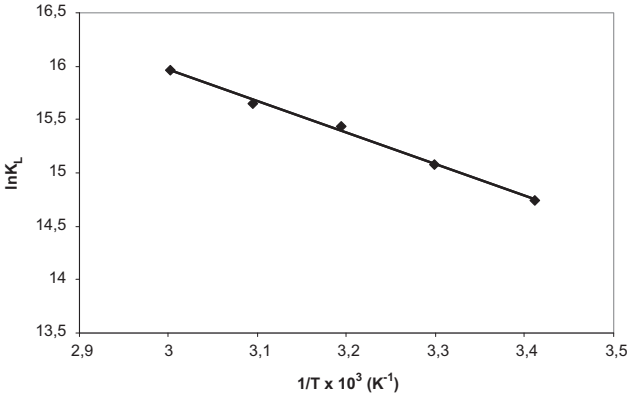

Fig. 6. Plot of ln K_L vs. $1/T$ for BY 28 adsorption onto sepiolite.

the free energy for the physisorption process is typically –20 and 0 kJ mol^{-1}, whereas that for the chemisorption process is in the range of −80 to –400 kJ mol^{-1} [59]. The overall free energy change during the adsorption process was negative for the experimental range of temperatures (Table 8), corresponding to a spontaneous physical process of BY 28 adsorption.

The positive value of ΔH^* suggests the endothermic nature of the adsorption process. The upper limit of the change of enthalpy for physisorption is generally 80 kJ mol^{-1}; the chemisorption is in the range of 80–420 kJ mol^{-1} [60]. The positive value of the enthalpy change (+24.53 kJ mol^{-1}) indicates that the adsorption process is endothermic, and this value also indicates that the adsorption follows a physisorption mechanism in nature involving weak forces of attraction between the adsorbed dye ions and sepiolite.

The reorientation or restructuring of the water molecules around the nonpolar solutes or surfaces is very unfavorable in terms of entropy because it disturbs the existing water structure and imposes a new and less ordered structure on the surrounding water molecules [61]. The number of water molecules surrounding the dye molecules decreases due to the adsorption of BY 28 onto the sepiolite, and thus, the degree of freedom of the water molecules increases. Therefore, the positive value of ΔS^* suggests that an increased randomness at the solid/solution interface occurred during the adsorption of BY 28 onto the sepiolite.

The pseudo-second-order rate constants were also determined using the different temperature values. The value of the rate constants increased from 3.74×10^{-2} to 9.99×10^{-2} g mg^{-1} min^{-1} with an increase in the solution temperature from 20 to 60℃ (Table 6), indicating that the adsorption of BY 28 onto the sepiolite was rate controlled.

The Arrhenius activation energy (E_a) can be calculated by Eq. (16) [30]:

Table 8
Thermodynamic parameters calculated from the Langmuir isotherm constant, K_L, for the adsorption of BY 28 onto sepiolite

T (℃)	ΔG^* (kJ mol^{-1})	ΔH^* (kJ mol^{-1})	ΔS^* (J mol^{-1} K^{-1})
20	–60.45	24.53	206.28
30	–62.51		
40	–64.57		
50	–66.63		
60	–68.69		

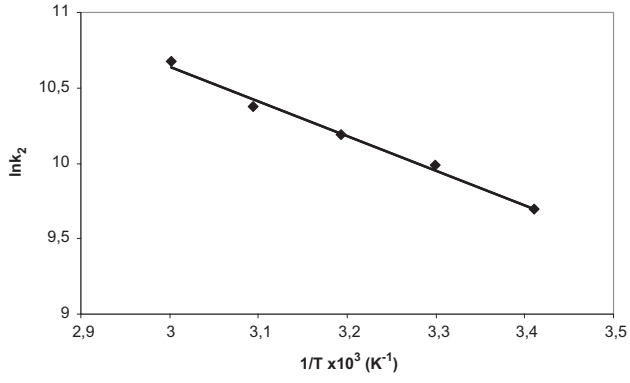

Fig. 7. Arrhenius plots for adsorption of BY 28.

Table 9
Comparison with some adsorbents of adsorption of BY 28

Adsorbent	Dye	Adsorption capacity (mg/g)	Experimental conditions			Reference
			I (M)	T (°C)	pH	
Clinoptilolite	BY 28	59.6	—	20	6–6.5	[63]
Amberlite XAD-4	BY 28	8.7	—	20	6–6.5	[63]
Bentonite	BY 28	230.8	—	20	6	[64]
Boron waste	BY 28	~74.8	—	25	6	[65]
Greeen alga	BY 28	27	—	–	8	[66]
Kaolin	BY 28	16.23	—	Room temperature	6	[67]
Sepiolite	BY 28	30.62	0.05	20	6	In this study

$$\ln k_2 = \ln A - \frac{E_a}{RT} \quad (16)$$

where A is the Arrhenius factor, and R is the gas constant. A linear plot of ln k_2 vs. $1/T$ for the adsorption of BY 28 onto the sepiolite was constructed to generate the E_a value from the slope (Fig. 7), resulting in an E_a value of 19.11 J mol^{-1} with a linear regression coefficient of 0.9911.

The magnitude of the activation energy indicates whether the adsorption is primarily a physical or a chemical process. A low activation energy value (5–40 kJ mol^{-1}) is characteristic of a physisorption process, whereas a high activation energy value (40–800 kJ mol^{-1}) suggests a chemisorption process [62]. The E_a value that was obtained for the adsorption of BY 28 onto the sepiolite indicates that the adsorption has a potential barrier, corresponding to a physisorption process (Fig. 6). Therefore, the affinity of the BY 28 for the sepiolite may be ascribed to electrostatic attractions, van der Waals forces, or hydrogen bonds between the dye and the surface of the particles.

3.5. Comparison of adsorbents for BY 28 adsorption

The maximum adsorption values for the adsorption of the BY 28 onto the sepiolite in the present study were compared with other adsorbents that are listed in Table 9. The results in Table 9 reveal that the sepiolite shows good potential as an adsorbent for the removal of the BY 28 from aqueous solutions.

4. Conclusions

The process conditions for the adsorption of the BY 28 dye onto the sepiolite as an economical sorbent were determined using RSM. The aim of this study was to investigate the interactive and primary effects of the initial pH, temperature, and ionic strength parameters on the amount of adsorbed dye. The planning of the experiments and the analysis of the results were performed by CCD. In this batch process, the interaction between the temperature and the ionic strength played an important role in the adsorption of the dye. The proposed quadratic model agrees well with the experimental data and with the determination coefficient (R^2 adj) of 98.52%. The optimum conditions were identified as an initial pH of 6 and a temperature of 25°C. The adsorption of the BY 28 onto the sepiolite was not affected by an ionic strength of up to 0.1 mol L^{-1} NaCl. The predicted amount of the adsorbed dye was 31.54 ± 0.05 (mg g^{-1}) at a 5% significance level. It was found that the q_e values calculated from the factorial experiment given in Table 3 show very low variation. Therefore, the adsorption process of BY 28 onto the sepiolite surface can be performed with natural pH levels, in dye solutions without salt, and at room temperature. After kinetic evaluation, the pseudo-second-order kinetic reaction model was found to be the better correlation of the data for dye removal. The intra-particle diffusion model was applied and it was found that external mass transfer is only significant for the initial period of time. Intra-particle diffusion controlled the adsorption rate at the final stage. The isotherm data were correlated better by the Langmuir isotherm model, and the maximum adsorption capacities were calculated in the range of 25.19–28.01 mg/g at different temperatures. Thermodynamic parameters suggested that the dye uptake by sepiolite was endothermic in nature. Based on the results, it was concluded that sepiolite has significant potential for removing basic dye from wastewater using the adsorption method.

References

[1] A.M. Talarposhti, T. Donnelly, G.K. Anderson, Colour removal from a simulated dye wastewater using a two-phase anaerobic packed bed reactor, Water Res. 35 (2001) 425–432.

[2] S. Şen, G.N. Demirer, Anaerobic treatment of real textile wastewater with a fluidized bed reactor, Water Res. 37 (2003) 1868–1878.
[3] B. Manu, S. Chaudhari, Anaerobic decolorisation of simulated textile wastewater containing azo dyes, Bioresour. Technol. 82 (2002) 225–231.
[4] K. Murugesan, I.H. Nam, Y.M. Kim, Y.S. Chang, Decolorization of reactive dyes by a thermostable laccase produced by *Ganoderma lucidum* in solid state culture, Enzyme Microb. Technol. 40 (2007) 1662–1672.
[5] B. Karagozoglu, M. Tasdemir, E. Demirbas, M. Kobya, The adsorption of basic dye (Astrazon Blue FGRL) from aqueous solutions onto sepiolite, fly ash and apricot shell activated carbon: Kinetic and equilibrium studies, J. Hazard. Mater. 147 (2007) 297–306.
[6] M. Tekbaş, N. Bektaş, H.C. Yatmaz, Adsorption studies of aqueous basic dye solutions using sepiolite, Desalination 249 (2009) 205–211.
[7] D. Bingöl, S.K. Bozbaş, Removal of lead (II) from aqueous solution on multiwalled carbon nanotube by using response surface methodology, Spectrosc. Lett. 45 (2012) 324–329.
[8] D. Bingöl, S. Veli, S. Zor, U. Özdemir, Analysis of adsorption of reactive azo dye onto $CuCl_2$ doped polyaniline using Box–Behnken design approach, Synth. Met. 162 (2012) 1566–1571.
[9] D. Bingöl, Removal of cadmium (ii) from aqueous solutions using a central composite design, Fresen. Environ. Bull. 20(10a) (2011) 2704–2709.
[10] D. Bingol, N. Tekin, M. Alkan, Brilliant Yellow dye adsorption onto sepiolite using a full factorial design, Appl. Clay Sci. 50 (2010) 315–321.
[11] C. Cojocaru, G.Z. Trznadel, Response surface modeling and optimization of copper removal from aqua solutions using polymer assisted ultrafiltration, J. Membr. Sci. 298 (2007) 56–70.
[12] S.H. Hasan, P. Srivastava, M. Talat, Biosorption of Pb (II) from water using biomass of *Aeromonas hydrophila*: Central composite design for optimization of process variables, J. Hazard. Mater. 168 (2009) 1155–1162.
[13] V. Jaikumar, V. Ramamurthi, Statistical analysis and optimization of acid dye biosorption by brewery waste biomass using response surface methodology, Mod. Appl. Sci. 3 (2009) 71–84.
[14] Y.L. Lai, G. Annadurai, F.C. Huang, J.F. Lee, Biosorption of Zn(II) on the different Ca-alginate beads from aqueous solution, Bioresour. Technol. 99(14) (2008) 6480–6487.
[15] K. Ravikumar, S. Krishnan, S. Ramalingam, K. Balu, Optimization of process variables by the application of response surface methodology for dye removal using a novel adsorbent, Dyes Pigm. 72 (2007) 66–74.
[16] Ş. Sert, M. Eral, Uranium adsorption studies on aminopropyl modified mesoporous sorbent (NH_2–MCM-41) using statistical design method, J. Nucl. Mater. 406 (2010) 285–292.
[17] M. Zarei, A. Niaei, D. Salari, A. Khataee, Application of response surface methodology for optimization of peroxi-coagulation of textile dye solution using carbon nanotube–PTFE cathode, J. Hazard. Mater. 173 (2010) 544–551.
[18] E. Eren, B. Afsin, Investigation of a basic dye adsorption from aqueous solution onto raw and pre-treated sepiolite surfaces, Dyes Pigm. 73 (2007) 162–167.
[19] I.A. Aguayo-Villarreal, L.A. Ramírez-Montoya, V. Hernández-Montoya, A. Bonilla-Petriciolet, M.A. Montes-Morán, E.M. Ramírez-López, Sorption mechanism of anionic dyes on pecan nut shells (Carya illinoinensis) using batch and continuous systems, Ind. Crops Prod. 48 (2013) 89–97.
[20] R. Fonseca-Correa, L. Giraldo, J.C. Moreno-Piraján, Trivalent chromium removal from aqueous solution with physically and chemically modified corncob waste, J. Anal. Appl. Pyrolysis 101 (2013) 132–141.
[21] N. Gupta, A.K. Kushwaha, M.C. Chattopadhyaya, Adsorption studies of cationic dyes onto Ashoka (Saraca asoca) leaf powder, J. Taiwan Inst. Chem. Eng. 43 (2012) 604–613.
[22] S. Mona, A. Kaushik, C.P. Kaushik, Biosorption of reactive dye by waste biomass of Nostoc linckia, Ecol. Eng. 37 (2011) 1589–1594.
[23] C.-Y. Tan, G. Li, X.-Q. Lu, Z.-L. Chen, Biosorption of Basic Orange using dried A. filiculoides, Ecol. Eng. 36 (2010) 1333–1340.
[24] S. Karaca, A. Gürses, Ö. Açışlı, A. Hassani, M. Kıranşan, K. Yıkılmaz, Modeling of adsorption isotherms and kinetics of Remazol Red RB adsorption from aqueous solution by modified clay, Desalin. Water Treat. 51 (2013) 2726–2739.
[25] E. Eren, O. Cubuk, H. Ciftci, B. Eren, B. Caglar, Adsorption of basic dye from aqueous solutions by modified sepiolite: Equilibrium, kinetics and thermodynamics study, Desalination 252 (2010) 88–96.
[26] M.M. Nassar, M.S. El-Geundi, A.A. Al-Wahbi, Equilibrium modeling and thermodynamic parameters for adsorption of cationic dyes onto Yemen natural clay, Desalin. Water Treat. 44 (2012) 340–349.
[27] E. Sabah, M.S. Çelik, Interaction of pyridine derivatives with sepiolite, J. Colloid Interf. Sci. 251 (2002) 33–38.
[28] F. Bergaya, M. Jaber, J.F. Lambert, Clays and clay minerals, in: M. Galimberti (Ed.), Rubber-Clay Nanocomposites: Science, Technology, and Applications, Wiley, Hoboken, NJ, 2011 (Chapter 1), pp. 3–44.
[29] G. Rytwo, D. Tropp, C. Serban, Adsorption of diquat, paraquat and methyl green on sepiolite: Experimental results and model calculations, Appl. Clay Sci. 20 (2002) 273–282.
[30] M. Alkan, M. Doğan, Y. Turhan, Ö. Demirbaş, P. Turan, Adsorption kinetics and mechanism of maxilon blue 5G dye on sepiolite from aqueous solutions, Biochem. Eng. J. 139(2) (2008) 213–223.
[31] A. Özcan, E.M. Öncü, A.S. Özcan, Kinetics, isotherm and thermodynamic studies of adsorption of Acid Blue 193 from aqueous solutions onto natural sepiolite, Colloids Surf. A 277(1–3) (2006) 90–97.
[32] S.C.R. Santos, R.A.R. Boaventura, Adsorption modelling of textile dyes by sepiolite, Appl. Clay Sci. 42 (2008) 137–145.
[33] E. Demirbas, M.Z. Nas, Batch kinetic and equilibrium studies of adsorption of Reactive Blue 21 by fly ash and sepiolite, Desalination 243 (2009) 8–21.
[34] İ. Küncek, S. Şener, Adsorption of methylene blue onto sonicated sepiolite from aqueous solutions, Ultrason. Sonochem. 17 (2010) 250–257.
[35] M. Alkan, Ö. Demirbaş, M. Doğan, Electrokinetic properties of sepiolite suspensions in different electrolyte media, J. Colloid Interf. Sci. 281 (2005) 240–248.

[36] M. Alkan, O. Demirbas, M. Doğan, Removal of acid yellow 49 from aqueous solution by adsorption, Fresenius Environ. Bull. 13(11a) (2004) 1112–1121.
[37] N. Tekin, A. Dinçer, Ö. Demirbaş, M. Alkan, Adsorption of cationic polyacrylamide onto sepiolite, J. Hazard. Mater. 134 (2006) 211–219.
[38] D. Baş, İ.H. Boyacı, Modeling and optimization I: Usability of response surface methodology, Int. J. Food Eng. 78 (2007) 836–845.
[39] K.P. Singh, S. Gupta, A.K. Singh, S. Sinha, Experimental design and response surface modeling for optimization of Rhodamine B removal from water by magnetic nanocomposite, Chem. Eng. J. 165 (2010) 151–160.
[40] D.C. Montgomery, Design and Analysis of Experiments, 7th ed., Wiley, New York, NY, 2008.
[41] A. Tsimpliaraki, S. Svinterikos, I. Zuburtikudis, S.I. Marras, C. Panayiotou, Nanofibrous structure of nonwoven mats of electrospun biodegradable polymer nanocomposites a design of experiments (DoE) study, Ind. Eng. Chem. Res. 48 (2009) 4365–4374.
[42] J. Zolgharnein, A. Shahmoradi, M.R. Sangi, Optimization of Pb(II) biosorption by Robinia tree leaves using statistical design of experiments, Talanta 76 (2008) 528–532.
[43] A. Tabak, E. Eren, B. Afsin, B. Caglar, Determination of adsorptive properties of a Turkish Sepiolite for removal of Reactive Blue 15 anionic dye from aqueous solutions, J. Hazard. Mater. 161 (2009) 1087–1094.
[44] M. Alkan, Ö. Demirbaş, S. Çelikçapa, M. Doğan, Sorption of acid red 57 from aqueous solution onto sepiolite, J. Hazard. Mater. 116 (2004) 135–145.
[45] M. Doğan, Y. Özdemir, M. Alkan, Adsorption kinetics and mechanism of cationic methyl violet and methylene blue dyes onto sepiolite, Dyes Pigm. 75 (2007) 701–713.
[46] M. Espinosa-Jimenez, R. Perea-Carpio, R. Padilla-Weigand, A. Ontiversos, Electrokinetic and thermodynamic analysis of the dyeing process of polyamide fabric with mordant black 17, J. Colloid Interf. Sci. 238 (2001) 33–36.
[47] Y.S. Ho, G. McKay, Pseudo-second order model for sorption processes, Process Biochem. 34 (1999) 451–465.
[48] M. Özacar, İ.A. Şengil, A kinetic study of metal complex dye sorption onto pine sawdust, Process Biochem. 40 (2005) 565–572.
[49] H. Chen, A. Wang, Kinetic and isothermal studies of lead ion adsorption onto palygorskite clay, J. Colloid Interface Sci. 307 (2007) 309–316.
[50] W.J. Weber, J.C. Morris, Advances in water pollution research: Removal of biologically resistant pollutant from wastewater by adsorption, in: Proceedings of 1st International Conference on Water Pollution Symposium, 2 (1962), Pergamon Press, Oxford, 231–266.
[51] Y.S. Ho, G. McKay, The kinetics of sorption of basic dyes from aqueous solution by sphagnum moss peat, Can. J. Chem. Eng. 76 (1998) 822–827.
[52] W.J. Weber, J.C. Morris, Kinetics of adsorption on carbon from solution, J. Sanit. Eng. Div. ASCE 89(SA2) (1963) 31–59.
[53] Y.S. Ho, G. McKay, Sorption of dyes and copper ions onto biosorbents, Process Biochem. 38 (2003) 1047–1061.
[54] Y. Önal, C. Akmil-Başar, D. Eren, Ç. Sarıcı-Özdemir, T. Depci, Adsorption kinetics of malachite green onto activated carbon prepared from tunçbilek lignite, J. Hazard. Mater. 128 (2006) 150–157.
[55] X. Xu, B.Y. Gao, X. Tang, Q.Y. Yue, Q.Q. Zhong, Q. Li, Characteristics of cellulosic amine-crosslinked copolymer and its sorption properties for Cr(VI) from aqueous solutions, J. Hazard. Mater. 189 (2011) 420–426.
[56] I. Langmuir, The adsorption of gases on plane surfaces of glass, mica and platinum, JACS 40 (1918) 1361–1403.
[57] H.M.F. Freundlich, Over the adsorption in solution, J. Phys. Chem. 57 (1906) 385–471.
[58] K.R. Hall, L.C. Eagleton, A. Acrivos, T. Vermeulen, Pore and solid diffusion kinetics fixed bed adsorption under constant pattern conditions, Ind. Eng. Chem. Res. Fund. 5 (1996) 212–213.
[59] A. Özcan, Ç. Ömeroğlu, Y. Erdoğan, A.S. Özcan, Modification of bentonite with a cationic surfactant: An adsorption study of textile dye Reactive Blue 19, J. Hazard. Mater. 140(1–2) (2007) 173–179.
[60] M. Şölener, S. Tunali, A.S. Özcan, A. Özcan, T. Gedikbey, Adsorption characteristics of lead(II) ions onto the clay/poly(methoxyethyl)acrylamide (PMEA) composite from aqueous solutions, Desalination 223 (2008) 308–322.
[61] N. Tekin, E. Kadıncı, Ö. Demirbaş, M. Alkan, A. Kara, Adsorption of polyvinylimidazole onto kaolinite, J. Colloid Interface Sci. 296 (2006) 472–479.
[62] H. Nollet, M. Roels, P. Lutgen, P. Van der Meeren, W. Verstraete, Removal of PCBs from wastewater using fly ash, Chemosphere 53(6) (2003) 655–665.
[63] J. Yener, T. Kopac, G. Dogu, T. Dogu, Adsorption of Basic Yellow 28 from aqueous solutions with clinoptilolite and amberlite, J. Colloid Interface Sci. 294 (2006) 255–264.
[64] M. Turabik, Adsorption of basic dyes from single and binary component systems onto bentonite: Simultaneous analysis of Basic Red 46 and Basic Yellow 28 by first order derivative spectrophotometric analysis method, J. Hazard. Mater. 158 (2008) 52–64.
[65] A. Olgun, N. Atar, Equilibrium and kinetic adsorption study of Basic Yellow 28 and Basic Red 46 by a boron industry waste, J. Hazard. Mater. 161 (2009) 148–156.
[66] V.K. Gupta, Application of low-cost adsorbents for dye removal—A review, J. Environ. Manage. 90 (2009) 2313–2342.
[67] A.R. Tehrani-Bagha, H. Nikkar, N.M. Mahmoodi, M. Markazi, F.M. Menger, The sorption of cationic dyes onto kaolin: Kinetic, isotherm and thermodynamic studies, Desalination 266 (2011) 274–280.